

GaP(001) and InP(001): Reflectance anisotropy and surface geometry

N. Esser

Institut für Festkörperphysik, Technische Universität Berlin, Hardenbergstrasse 36, 10623 Berlin, Germany

W. G. Schmidt and J. Bernholc

Department of Physics, North Carolina State University, Raleigh, North Carolina 27695-8202

A. M. Frisch,^{a)} P. Vogt, M. Zorn, M. Pristovsek, and W. Richter

Institut für Festkörperphysik, Technische Universität Berlin, Hardenbergstrasse 36, 10623 Berlin, Germany

F. Bechstedt

Institut für Festkörpertheorie und Theoretische Optik, Friedrich-Schiller-Universität, Max-Wien-Platz 1, 07743 Jena, Germany

Th. Hannappel and S. Visbeck

Hahn-Meitner Institut, CD, Glienickestr. 100, 14109 Berlin, Germany

(Received 20 January 1999; accepted 30 March 1999)

We have investigated the optical anisotropy of GaP(001) and InP(001) surfaces. The samples were prepared by homoepitaxial metalorganic vapor phase epitaxy growth and either directly transferred into ultrahigh vacuum (UHV) or *in situ* capped and, after transfer, decapped in UHV by thermal desorption of a P/As capping layer. Symmetry, composition, and surface optical anisotropy were characterized by low-energy electron diffraction, Auger electron spectroscopy, and reflectance anisotropy spectroscopy. We observe $(2 \times 1)/(2 \times 2)$ -like reconstructions for the very P-rich and (2×4) reconstructions for the more cation-rich surfaces. No (4×2) reconstruction could be prepared, independent of the preparation method. A comparison of the reflectance anisotropy between GaP(001) and InP(001) surfaces shows similar line shapes for the very cation-rich (2×4) surfaces. For less cation-rich surfaces, however, we observe distinct differences between the spectra of the two systems. In both cases, different line shapes in the reflection anisotropy spectra occur for the (2×4) periodicity, suggesting the existence of different (2×4) geometries. The experimental results are discussed on the background of atomic structures, total energies and reflectance anisotropy spectra obtained *ab initio* from density-functional theory local-density approximation calculations. © 1999 American Vacuum Society. [S0734-211X(99)03504-0]

I. INTRODUCTION

Much progress has been made in recent years in understanding the microscopic structure of the growth planes of III-V compound semiconductors (for a recent review, see, e.g., Ref. 1). Optical anisotropy at the same time has been proven to be an additional and complementary tool to electron spectroscopic methods for investigating the microscopic surface structure of semiconductors.^{2,3} Previous investigations of GaAs(001)^{4,5} and InP(001)⁶ surfaces have shown that the atomic structure can be successfully clarified in many cases by comparing total energy and band structure calculations for the optical anisotropy on the one hand with experimental data of the optical anisotropy on the other hand. The atomic surface structures of the (2×4) -GaP(001) and -InP(001) surfaces were recently investigated by density functional theory local-density approximation (DFT-LDA) total energy calculations.^{7,8} As in the case of InP(001), the atomic structures of GaP(001) were found to be different from the well-investigated GaAs(001) surface,⁹⁻¹¹ due to a large size difference between cations and anions.

While several recent studies have addressed the atomic structure of InP(001),^{8,12-14} much less is known about

GaP(001). Available experimental studies lead to different and partially contradictive conclusions about the symmetry and structure of the GaP(001) surface. So far it has been suggested mostly that ion bombardment and annealing as well as decapping of GaP(001) results in a $(4 \times 2)/c(8 \times 2)$ reconstructed, Ga-rich surface,¹⁵⁻²¹ in analogy to the corresponding Ga-rich GaAs(001) surface structure.⁹ In a more recent investigation by ion scattering,²² however, a (2×4) symmetry was reported. Similar ambiguous results for GaP(001) can be found in literature for gas source molecular beam epitaxy (MBE) experiments: In Ref. 23 it is reported that (2×4) and (4×2) reconstruction pattern correspond to P- and Ga-stabilized surfaces, whereas in Ref. 24, a (2×4) reconstruction was observed under Ga as well as under P supply. Additionally, the authors of Ref. 24 found an intermediate (4×4) reconstruction during layer growth and suggested the formation of Ga droplets on a (2×4) reconstructed surface for high amounts of Ga supply. Only few data can be found in literature about the optical anisotropy of GaP(001). To our knowledge, there exist studies of GaP(001) surfaces in MBE, metalorganic vapor phase epitaxy (MOVPE) and chemical beam epitaxy (CBE).²⁵⁻²⁸ Apart from Ref. 7 no reflectance anisotropy data for GaP(001) surfaces in ultrahigh vacuum (UHV) are available.

In the present study, clean and well-ordered (001) sur-

^{a)}Electronic mail: frisch@gift.physik.tu-berlin.de

faces of MOVPE-grown GaP and InP with different stoichiometries are prepared under ultrahigh vacuum conditions. All samples are characterized by low-energy electron diffraction (LEED), Auger electron spectroscopy (AES), and reflectance anisotropy spectroscopy (RAS). Based on total-energy (TE) calculations and by comparison of experimental data to calculated optical anisotropies for various atomic structure models it is shown that several (2×4) reconstructions exist for GaP(001) and InP(001). They realize different stoichiometries. (4×2) structures do not occur in either case.

II. METHOD

The GaP(001) surfaces were prepared by thermal desorption of a protective arsenic/phosphorus double layer (cap) under UHV conditions. For this purpose, homoepitaxial GaP epilayers were grown by MOVPE on highly *n*-doped (10^{18} cm^{-3}) GaP(001) substrates and capped *in situ* utilizing the photodecomposition of phosphine and arsine by an excimer laser source.^{27,29(a)} The thermal desorption of the protective arsenic/phosphorus layer was performed at 690 K in UHV at a base pressure $\leq 10^{-10}$ hPa. The InP(001) samples were grown by MOVPE on *n*-doped (10^{17} cm^{-3}) InP(001) substrates and transferred under UHV conditions in the analyzing UHV chamber directly after growth, without using the capping technique.^{29(b)} Starting with P-rich surface conditions in either case, different reconstructions were prepared by subsequent annealing in UHV. After cooling to room temperature, the surfaces were investigated by LEED, RAS, and AES.

The calculations were based on DFT-LDA. Optical properties are calculated in independent-particle approximation from the DFT-LDA electronic structure. To determine the optical anisotropy, we follow the formalism developed by Del Sole³⁰ and Manghi *et al.*³¹ Computational details can be found in Refs. 6 and 11.

III. RESULTS AND DISCUSSION

A. Surface symmetry and composition

The decapped GaP(001) surfaces (after annealing to 690 K) show a $(2 \times 1)/(2 \times 2)$ -like LEED pattern [see Fig. 1(a)], with clear (2×1) spots plus additional streaks in the $[110]$ half order position. A similar LEED pattern [see Fig. 1(b)] is observed from InP(001) surfaces, directly after transfer into the UHV system. Annealing to 785 and 645 K leads to (2×4) LEED patterns for GaP(001) as well as for InP(001). The LEED pattern of the (2×4) GaP(001) surface does not allow us to distinguish between a (2×4) and a $(2 \times 4)/c(2 \times 8)$ reconstruction [Fig. 1(c)] due to not fully resolved fractional order spots in the $[110]$ direction. The LEED pattern of the InP(001) surface, on the contrary, shows a (2×4) periodicity, or a superposition of $(2 \times 1)/(2 \times 2)$ and (2×4) [Fig. 1(d)]. Upon further annealing up to 1000 K the quality of the LEED pattern for GaP(001) is improved and the former streaks develop into sharp spots indicating a pure (2×4) reconstruction, similar to the pattern observed for InP(001) [Figs. 1(e) and 1(f)]. Upon an-

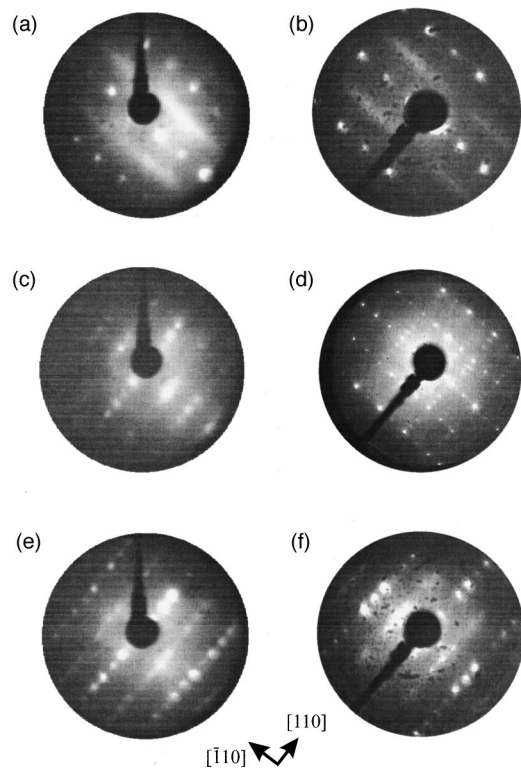


FIG. 1. LEED pattern recorded from GaP(001) and InP(001): (a) $(2 \times 1)/(2 \times 2)$ GaP(001) taken at a electron energy of 53 eV, (b) $(2 \times 1)/(2 \times 2)$ InP(001) (electron energy 50 eV), (c) P-rich (2×4) GaP(001) (electron energy 56 eV), (d) (2×4) InP(001) (electron energy 120 eV), (e) Ga-rich (2×4) GaP(001) (electron energy 52 eV), (f) InP(001) (electron energy 50 eV).

nealing to still higher temperatures [≥ 1000 K for GaP(001) and ≥ 725 K for InP(001)] the symmetry of the LEED patterns remains unchanged until the surfaces deteriorate by forming Ga or In droplets, as indicated by a metallic component in the Ga $3d$ /In $4d$ core level photoemission lines (not shown here). AES measurements performed on GaP after decapping and InP after UHV transfer show no detectable carbon or oxygen contaminations. Moreover, the composition of the GaP(001) surfaces was examined. The P/Ga ratio for the $(2 \times 1)/(2 \times 2)$ -like GaP(001) surface shows P-rich surface conditions, but it cannot be exactly determined because of the P desorption induced by the electron beam. On the (2×4) reconstructed GaP(001) surface at low annealing temperatures (only slightly above 785 K), the P/Ga intensity ratio is close to the one of the GaP(110) cleavage face (balanced stoichiometry). Upon annealing to higher temperatures (1000 K) the ratio changes successively by a factor of approximately two towards a Ga-rich surface, suggesting the existence of a more P-rich (2×4) at lower and a Ga-rich (2×4) reconstruction at higher annealing temperatures.

B. Optical anisotropy: Experimental results

Real parts of different RAS spectra recorded from GaP(001) and InP(001) surfaces are shown in Fig. 2. For comparison, a RAS spectrum of the $\beta 2(2 \times 4)$ GaAs(001) is

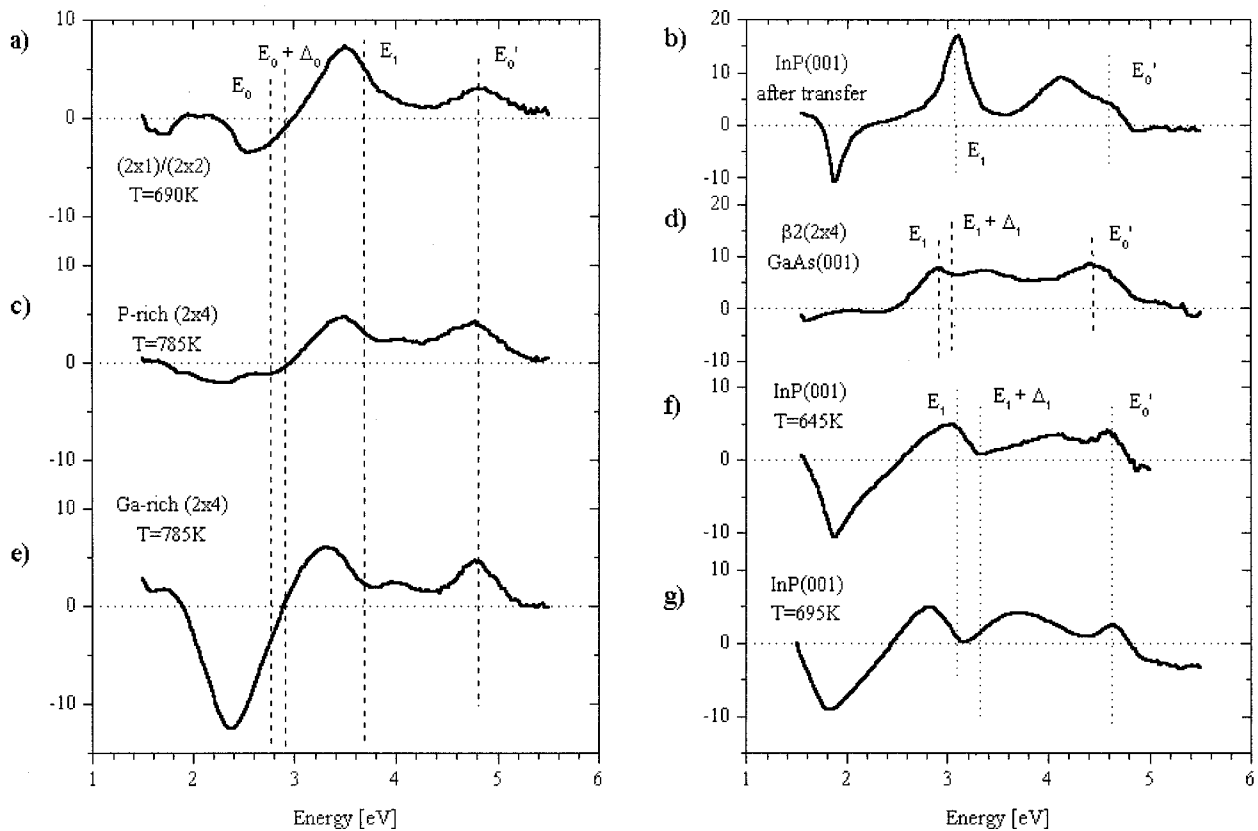


FIG. 2. Real parts of $((r_{\bar{1}10}r_{110})/\langle r \rangle) \times 10^3$ (LEED patterns and annealing temperatures are indicated in the plot) for: GaP(001) [left panel, (a), (c), (e)] InP(001) [right panel, (b), (f), (g)], and $\beta 2(2 \times 4)$ GaAs(001) [right panel, (d)].

shown in Fig. 2(d). Three different spectral line shapes are reproducibly observed on GaP(001) and InP(001), correlated to the surface preparation: a characteristic line shape belongs to the $(2 \times 1)/(2 \times 2)$ -like structures [Figs. 2(a), 2(b)], and two different line shapes are observed in either case for (2×4) surface structures, one correlated to P-rich conditions at lower annealing temperature [Figs. 2(c), 2(f)] and one to cation-rich conditions at higher annealing temperature [Figs. 2(e), 2(g)].

The P-rich GaP(001) (2×4) surface [Fig. 2(b)] shows a spectrum which is qualitatively similar to the one observed for the As dimer terminated $\beta 2(2 \times 4)$ GaAs(001) surface.³⁻⁵ It is dominated by pronounced maxima at 3.5 and 4.8 eV, close to the E_1 and E'_0 gap energies of GaP (3.69 and 4.77 eV, respectively³²) and a weak maximum at 4 eV. The RAS spectrum of InP under comparable conditions has a different line shape: In addition to maxima around the bulk critical points E_1 and E'_0 (3.16 and 4.68 eV, respectively³³) a strong minimum at 1.9 eV shows up. We mention that in Ref. 34 a somewhat different spectrum (nearly no negative anisotropy) has been assigned to the P-rich phase of InP (2×4) . The reason for that difference is not clear at present. The line shapes shown in Figs. 2(f) and 2(g) are, however, reproducibly observed in our UHV experiments, whereas a line shape comparable to Ref. 34 could not be obtained in spite of repeated attempts. After annealing to higher temperatures the RAS spectra for GaP and InP(001) change and

become similar in line shape. New features in the GaP spectrum are a strong minimum at 2.4 eV and a maximum at 3.2 eV, significantly below the E_1 gap of GaP. On InP the first maximum shifts to somewhat lower energies and an additional maximum appears between E_1 and E'_0 . On both materials, the maximum at the E'_0 point remains unaffected.

Summarizing the experimental results, there are clear similarities between the very anion-rich $(2 \times 1)/(2 \times 2)$ -like and the very cation-rich (2×4) reconstructed GaP(001) and InP(001) surfaces, in particular, if one takes into account the different bulk critical point energies of the two materials. The spectrum of the P-rich (2×4) reconstructed GaP(001) surface, however, is distinct from the corresponding InP spectrum and resembles the one of GaAs(001) $\beta 2(2 \times 4)$. The evolution of the RAS spectra of GaP(001) with increasing Ga coverage of the surface implies that at least two distinct (2×4) structures with different stoichiometry exist on the GaP(001) surface. This conclusion cannot be drawn for InP(001) surfaces. Scanning tunneling microscopy images³⁵ imply that the transition structure corresponds to a two-domain surface composed of P-rich $(2 \times 1)/(2 \times 2)$ and In-rich (2×4) domains. Also the RAS spectrum [Fig. 2(f)] can be reproduced by a linear superposition of spectra 2(b) and 2(g).

C. Atomic structure of the surfaces

So far, only the (2×4) -surface atomic structures [especially for InP(001)] have been analyzed in detail, while the

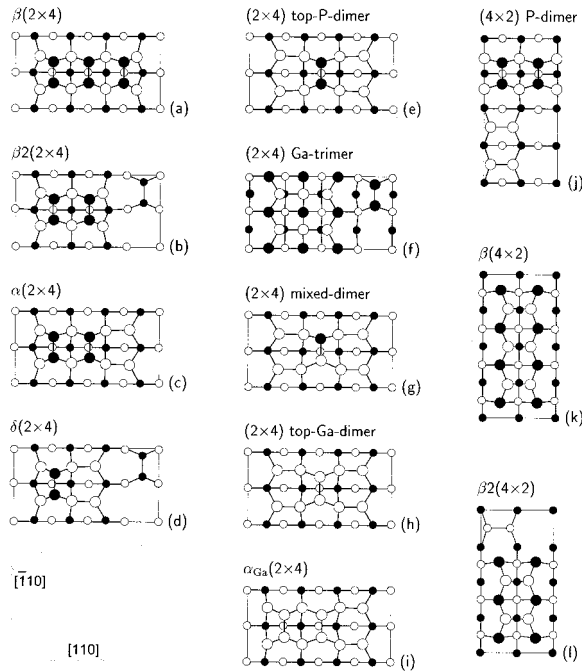


FIG. 3. Top view of relaxed GaP(001) (2×4) and (4×2) surface reconstruction models. Empty (filled) circles represent Ga (P) atoms. Large (small) symbols indicate positions in the first and second (third and fourth) atomic layers. (2×4) and (4×2) reconstructions are ordered by increasing Ga coverage.

structure of the $(2 \times 1)/(2 \times 2)$ -reconstructed surfaces is still completely unclear. STM and photoemission data are available for InP(001) (2×4) .^{8,13,29(a)} TE calculations performed on InP for a large variety of different (2×4) - and (4×2) -reconstruction models revealed a new type of dimer reconstruction involving mixed In–P surface dimers for In-rich surfaces, consistent with the experimental data.⁸ Very recently, TE calculations have also been performed for a series of structural models for GaP(001).⁷ Figure 3 shows the structural models considered for GaP. One of these models, the $\delta(2 \times 4)$ surface structure, which is believed to describe the Sb-induced GaAs (2×4) reconstruction,³⁶ turned out to be energetically favored for GaP(001), but was not considered in earlier studies on InP(001). We included that model in the present work.

The investigated models realize different In or Ga coverages and can therefore be compared energetically only by taking into account the chemical potentials of the surface constituents.¹¹ In Fig. 4 we show the relative formation energies of the considered surface structures vs the cation chemical potential for both InP(001) and GaP(001) surfaces. The phase diagrams show following fundamental similarities:

- (i) (2×4) structures represent the stable surfaces under cation-rich conditions, in contrast to the GaAs(001) case where (4×2) structures are known to exist under cation-rich conditions.
- (ii) A new atomic surface structure, consisting of mixed cation–P dimers adsorbed on top of a complete cation layer

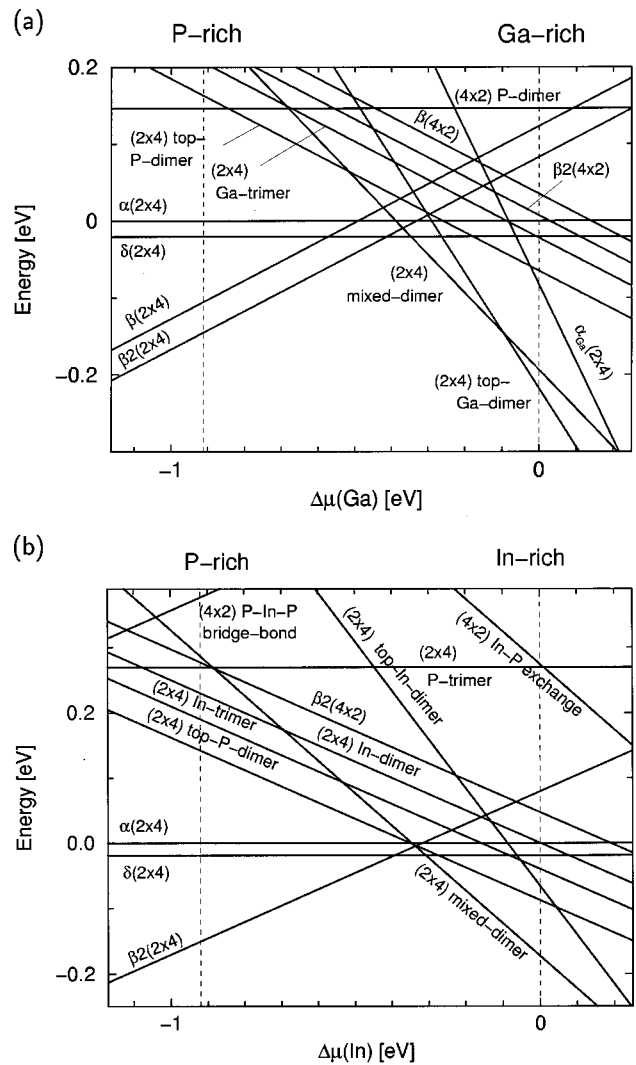


FIG. 4. (a) Relative formation energy per (1×1) unit cell for GaP(001) surface reconstructions vs $\Delta\mu(\text{Ga}) := \mu_{\text{bulk}}(\text{Ga}) - \mu(\text{Ga})$. The approximate thermodynamically allowed range: $-\Delta H_f(\text{GaP}) \leq \Delta\mu(\text{Ga}) \leq 0$ is indicated by dashed lines. (b) Same as in (a), but for InP(001) surface structures.

[Fig. 3(g)] represents the lowest energy structure over a prominent range of chemical potentials.

(iii) For a certain range of preparation conditions, the δ geometry [Fig. 3(d)] may occur. Given the limited accuracy of our calculations,¹¹ further structures such as α and top P dimer [Figs. 3(c) and 3(e)] cannot be excluded for the transition between cation- and anion-rich surfaces. Finally, under P-rich conditions P dimers in a $\beta 2(2 \times 4)$ geometry [Fig. 3(b)], as known from As-rich GaAs(001) surfaces,^{10,37} represent the lowest energy structure. However, this result must be taken with caution, since for P-rich conditions the experimental results indicate the appearance of $(2 \times 1)/(2 \times 2)$ structures on both GaP as well as InP, which were not considered in the TE calculations.

(iv) All equilibrium structures are in agreement with electron counting heuristics.³⁸

The similarity between the surface phase diagrams of InP and GaP points towards a common mechanism: The size

difference between anions and cations hinders the accommodation of sp^2 -hybridized cation dimer atoms that are typical for cation-rich GaAs(001) surfaces. Instead, the formation of single-dimer structures is favored for cation-rich surfaces.

Besides these similarities, however, there is also an obvious difference: On InP(001) the mixed-dimer structure appears to be the only stable geometry under In-rich conditions, while on GaP(001) the top-Ga dimer model [Fig. 3(h)] is lower in energy in the extreme cation-rich limit.

The phase diagrams of GaP and InP in Fig. 4 demonstrate the existence of different stable (2×4) surface phases depending on the value of the cation chemical potential, i.e., the surface preparation conditions. This finding is in excellent agreement with the qualitative evolution of the surface optical anisotropy on GaP(001).

Since RAS as an optical technique is applicable in UHV as well as gas phase surroundings, the dependence of InP and GaP surface structures on different environments (e.g., growth conditions in MOVPE, MBE, CBE, and UHV) can be addressed by comparing the RAS spectra taken under different conditions. Comparing our spectra with the ones taken in MOVPE and CBE reveal, that for InP as well as for GaP, the same line shapes occur in the different environments.^{26–28,39} Moreover, an excellent agreement between symmetry observed by RHEED in CBE^{28,39} and LEED in our UHV experiments is found in both InP and GaP cases. There is, however, one exception: A $\beta 2(2 \times 4)$ seemingly observed in MBE for InP(001)³⁴ is not showing up in our experiments.

D. Optical anisotropy: Calculation

As shown above, the evolution of the surface optical anisotropy and the calculated equilibrium surface structures is qualitatively consistent. An even more direct comparison between theory and measurement, however, is desirable in order to identify specific surface structures. To this end, we compare the computed surface reflectance anisotropy of the energetically favored structures with the experimental RAS spectra.

Simulated spectra for GaP(001) are shown in the upper panel of Fig. 5.⁷ Earlier we have shown that surface related transitions dominate the low-energy part while bulk-related transitions are more pronounced in the high-energy part of the RAS spectra.⁷ The top-Ga dimer, mixed dimer, and δ structures show a pronounced negative anisotropy in the low-energy region, with minima between 2.0 and 2.3 eV. The strength of that anisotropy is directly correlated to the number of Ga–Ga bonds along the $[110]$ direction. Its magnitude is the highest for the top-Ga-dimer model with eight bonds, slightly reduced and shifted to lower energies for the mixed-dimer geometry with six cation–cation bonds and flattened for the δ structure with only two such bonds.

The positive anisotropy in the high energy region of the spectra is correlated to the formation of P–P dimers oriented along $[\bar{1}10]$: For the $\beta 2$ geometry with three P–P dimers, we find a relatively strong positive anisotropy between about 2.4 and 4.4 eV. The shape of that anisotropy is roughly preserved for the δ structure, featuring one P–P dimer, however,

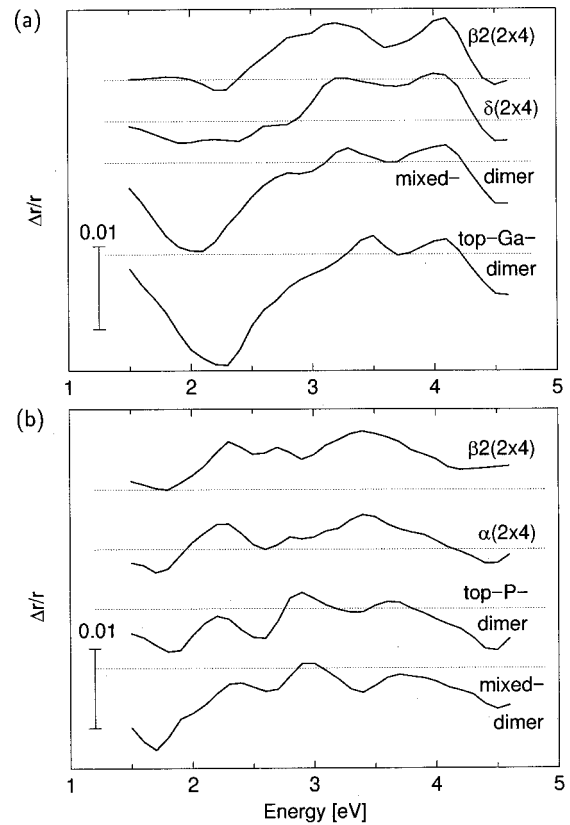


Fig. 5. (a) RAS spectra (same convention as in Fig. 2) calculated for the energetically favored structural models of the GaP(001) (2×4) surface. The zero line in each spectrum is indicated by a horizontal dotted line. (b) Same as in (a), but for InP(001) surface structures.

with reduced magnitude and the spectrum is shifted down. An even further reduction in positive anisotropy occurs for the mixed-dimer and top-Ga-dimer structures (no P–P dimers).

According calculations for InP(001)⁶ are shown in the lower panel of Fig. 5. Similar systematic trends as for GaP(001) are observed in the optical anisotropy of InP(001): cation-rich surfaces show a characteristic strong minimum at low energies, P-dimer terminated ones a broad positive anisotropy at higher energies.

In fact, apart from some energy shift due to the neglect of many-body effects in DFT-LDA, the calculated spectra are in rather good agreement with the experimental optical anisotropy. Together with the calculated phase diagrams they allow a conclusive comparison. The RAS spectra measured for the (2×4) structures at higher annealing temperature (In/Ga-rich phases) feature a strong negative peak in the low-energy region. Given the energy position of this peak and its dependence on the preparation conditions, it can be identified with the calculated negative anisotropy arising from cation–cation surface bond related states. Both the top-Ga-dimer model and the mixed-dimer model thus are plausible candidates to explain the Ga-rich surface phase on GaP(001), while on InP the mixed-dimer model represents the only possible structure under In-rich conditions.

The measured spectrum for the GaP(001) (2×4) struc-

ture annealed at lower temperature (more P-rich phase) is dominated by a “camelback” overall spectrum shape with maxima between the energies of the E_0 and E_1 critical points and at the E'_0 bulk peak. No negative anisotropy appears. The only computed spectrum with no (or very little) negative anisotropy belongs to the $\beta 2(2 \times 4)$ structure. Maxima appear at 3.2 and 4.1 eV, close to the calculated energies of the E_1 and E'_0 critical points. Our results thus indicate that the less Ga-rich phase of the GaP(001) (2×4) surface corresponds to the $\beta 2(2 \times 4)$ structure known from As-rich GaAs(001) surfaces. This condition of a vanishing negative anisotropy is clearly not fulfilled in the case of the more P-rich InP(001) (2×4) structure. Consequently, this structure should be different, still containing In–In bonds in addition to P dimers. As mentioned above, a possible explanation would be a surface containing different domains.

IV. CONCLUSIONS

In conclusion, we have presented a comprehensive study of the optical anisotropy of GaP(001) and InP(001) surfaces based on the comparison of experimental results with calculated surface geometries and reflectance anisotropy spectra. Both for a balanced surface stoichiometry and for cation-rich conditions, we find (2×4) reconstructed surfaces that are stabilized by the formation of dimers. Experiment as well as theory suggest the existence of different (2×4) surface phases, depending on the cation content of the surface. Our results indicate that mixed dimers on top of an cation-terminated surface are the ground states of the Ga/In-rich phase of GaP(001) and InP(001) surfaces, consistent with previous findings for the InP(001) (2×4). For the less cation-rich surface phases, we suggest the formation of P–P dimers in a $\beta 2(2 \times 4)$ geometry for GaP(001). In case of InP, however, cation–cation bonds seem to be still present at the surface.

ACKNOWLEDGMENTS

Financial support by BMBF-Verbundprojekt 22, DFG (Schm 1361/1-1, Es 127/4-1), NSF (DMR 9408437), and ONR (N00014-96-I-0161) is gratefully acknowledged. This work was supported in part by grants of supercomputer time from the DoD Challenge Program and the North Carolina Supercomputer Center.

¹Q.-K. Xue, T. Hashizume, and T. Sakurai, *Prog. Surf. Sci.* **56**, 1 (1997), and references therein.

²W. Richter and J.-T. Zettler, *Appl. Surf. Sci.* **100/101**, 465 (1996).

³I. Kamiya, D. E. Aspnes, L. T. Florez, and J. P. Harbison, *Phys. Rev. B* **46**, 15894 (1992).

⁴M. Murayama, K. Shiraishi, and T. Nakayama, *Jpn. J. Appl. Phys., Part 1* **37**, 4109 (1998).

⁵A. I. Shkrebtii, N. Esser, W. Richter, W. G. Schmidt, F. Bechstedt, B. O. Fimland, A. Kley, and R. Del Sole, *Phys. Rev. Lett.* **81**, 721 (1998).

⁶W. G. Schmidt, E. Briggs, J. Bernholc, and F. Bechstedt, *Phys. Rev. B* **59**, 2234 (1999).

⁷A. M. Frisch, W. G. Schmidt, J. Bernholc, M. Pristovsek, N. Esser, and W. Richter, *Phys. Rev. B* (to be published).

⁸W. G. Schmidt, F. Bechstedt, N. Esser, M. Pristovsek, Ch. Schultz, and W. Richter, *Phys. Rev. B* **57**, 14596 (1998); W. G. Schmidt and F. Bechstedt, *Surf. Sci.* **409**, 474 (1998).

⁹D. K. Biegelsen, R. D. Bringans, J. E. Northrup, and L.-E. Swartz, *Phys. Rev.* **41**, 5701 (1990).

¹⁰J. E. Northrup and S. Froyen, *Mater. Sci. Eng., B* **30**, 81 (1995).

¹¹W. G. Schmidt, *Appl. Phys. A: Mater. Sci. Process.* **65**, 581 (1997).

¹²J. Kinsky, Ch. Schultz, D. Pahlke, A. M. Frisch, T. Herrmann, N. Esser, and W. Richter, *Appl. Surf. Sci.* **123**, 228 (1998).

¹³C. D. MacPherson, R. A. Wolkow, C. E. J. Mitchell, and A. B. McLean, *Phys. Rev. Lett.* **77**, 691 (1996).

¹⁴M. M. Sung, C. Kim, H. Bu, D. S. Karpuzov, and J. W. Rabalais, *Surf. Sci.* **322**, 116 (1995).

¹⁵Y. Fukuda, M. Shimomura, N. Sanada, and N. Nagoshi, *J. Appl. Phys.* **76**, 3632 (1994).

¹⁶N. Sanada, M. Shimomura, and Y. Fukuda, and T. Sato, *Appl. Phys. Lett.* **67**, 1432 (1995).

¹⁷A. Watanabe, H. Shimaya, M. Naitoh, and S. Nishigaki, *J. Vac. Sci. Technol. B* **14**, 3599 (1996).

¹⁸M. Naitoh, A. Watanabe, A. Konishi, and S. Nishigaki, *Jpn. J. Appl. Phys., Part 1* **35**, 4789 (1996).

¹⁹M. M. Sung and J. W. Rabalais, *Surf. Sci.* **365**, 136 (1996).

²⁰N. Oishi, F. Shoji, A. Konishi, M. Naitoh, and S. Nishigaki, *Surf. Rev. Lett.* **5**, 223 (1998).

²¹I. M. Vitomirov, A. Raisanen, L. J. Brillson, C. L. Lin, D. T. McInturff, P. D. Kirchner, and J. M. Woodall, *J. Vac. Sci. Technol. A* **11**, 841 (1993).

²²M. Naitoh, A. Konishi, H. Inenaga, S. Nishigaki, N. Oishi, and F. Shoji, *Surf. Sci.* **402-404**, 623 (1998).

²³J. N. Baillargeon, K. Y. Cheng, and K. C. Hsieh, *Appl. Phys. Lett.* **56**, 2201 (1990).

²⁴M. Yoshikawa, A. Nakamura, T. Nomura, and K. Ishikawa, *Jpn. J. Appl. Phys., Part 1* **35**, 1205 (1995).

²⁵P. A. Postigo, G. Armelles, and F. Briones, *Phys. Rev. B* **58**, 9659 (1998).

²⁶J. S. Luo, J. F. Geisz, J. M. Olson, and M. C. Wu, *J. Cryst. Growth* **174**, 558 (1997).

²⁷K. Knorr, M. Pristovsek, U. Resch-Esser, N. Esser, M. Zorn, and W. Richter, *J. Cryst. Growth* **170**, 230 (1997).

²⁸M. Zorn, B. Junno, T. Trepk, S. Bose, L. Samuelson, J.-T. Zettler, and W. Richter, *Phys. Rev. B* (submitted).

²⁹(a) N. Esser, U. Resch-Esser, M. Pristovsek, and W. Richter, *Phys. Rev. B* **53**, R13257 (1996); (b) Th. Hannappel, S. Visbeck, K. Knorr, J. Mahrt, M. Zorn, and F. Willig, *Appl. Phys. A: Mater. Sci. Process.* (in press).

³⁰R. Del Sole, *Solid State Commun.* **37**, 537 (1981).

³¹F. Manghi, R. Del Sole, A. Selloni, and E. Molinari, *Phys. Rev. B* **41**, 9935 (1990).

³²S. Zollner, M. Garriga, J. Kirchner, J. Humlicek, and M. Cardona, *Phys. Rev. B* **48**, 11 (1993).

³³P. Lautenschlager, M. Garriga, and M. Cardona, *Phys. Rev. B* **36**, 4813 (1987).

³⁴K. B. Ozanyan, P. J. Parbrook, M. Hopkinson, C. R. Whitehouse, Z. Sobiesierski, and D. I. Westwood, *J. Appl. Phys.* **82**, 474 (1997).

³⁵P. Vogt, Th. Hannappel, S. Visbeck, K. Knorr, N. Esser, and W. Richter, *Phys. Rev. B* (to be published).

³⁶W. G. Schmidt and F. Bechstedt, *Phys. Rev. B* **55**, 13051 (1997).

³⁷W. G. Schmidt and F. Bechstedt, *Phys. Rev. B* **54**, 16742 (1996).

³⁸M. D. Pashley, *Phys. Rev. B* **40**, 10481 (1989).

³⁹M. Zorn, T. Trepk, J.-T. Zettler, B. Junno, C. Meyne, K. Knorr, T. Wethkamp, M. Klein, M. Müller, W. Richter, and L. Samuelson, *Appl. Phys. A: Mater. Sci. Process.* **65**, 333 (1997).